A Monte Carlo Simulation for the Micellization of ABA- and BAB-Type Triblock Copolymers in a Selective Solvent

Seung Hyun Kim and Won Ho Jo*

Hyperstructured Organic Materials Research Center, and School of Materials Science and Engineering, Seoul National University, Seoul 151-742, Korea

Received March 26, 2001; Revised Manuscript Received July 11, 2001

ABSTRACT: The micellization behaviors of ABA and BAB triblock copolymers in a solvent selective for block A are investigated by means of grand canonical Monte Carlo (GCMC) simulation. The basic micellar parameters such as the micellar size, its distribution, the micellar shape, and the internal structure of micelles are obtained and compared for both systems. The critical micelle concentrations (cmc) are quantitatively estimated from the osmotic pressure obtained by the GCMC simulation combined with the multiple histogram method. The results of simulation show that the chain architecture of the triblock copolymers shows large differences in their association behavior in a selective solvent, although both copolymers have the same composition and total chain length. The thermodynamic analysis confirms that an additional entropy loss due to the looping conformation of the middle block of BAB copolymer induces a higher cmc value and therefore reduces the capability to self-assemble into micelles. As a result, the BAB copolymer chain may have various chain topology such as dangling, loop, and bridge chains in micelles. From the multiple equilibrium model, it is possible to extract the entropy associated with packing the chains into a micelle for two different systems. The BAB copolymer yields less negative packing entropy due to less order of micelles by the presence of the dangling and bridge chains as compared with ABA copolymer, which results in micelles with larger sizes and a broader size distribution despite its high cmc value.

1. Introduction

Amphiphilic copolymers such as diblock and triblock copolymers have been well-known to have an ability to self-assemble into micelles in a solvent which is selective for one of their constituents.[1−3] Analogous to the association of conventional and low molecular weight surfactants, the micelles of block copolymers consist of two phases: an inner core containing predominantly insoluble blocks and an outer corona containing both the soluble blocks and the solvent molecules. In most cases, these micelles have spherical shape and a narrow size distribution. However, it is important to note that there is some inherent complexity in the micellization of block copolymers when compared with the surfactants. For example, the micellization of block copolymers depends strongly on their block length, the composition (i.e., the block length ratio), the block architecture, etc. In this work, we mainly focus on the micellization behavior of triblock copolymers, particularly on the architecture effects of triblock copolymers on micellization.

Symmetrical triblock copolymers, although composed of the same chemical components, exhibit quite different association behavior in a selective solvent depending on their chain architecture. A large number of efforts have been made to clarify the micellization behavior of triblock copolymers by using the experiments,[4−14] theories,[15] and computer simulations.[16,17] However, there are only a few studies for a direct comparison of the micelle formation and the structural characteristics between two different triblock copolymer systems (viz., ABA and BAB triblock copolymers in a selective solvent for A blocks). Zhou and Chu[18] and Booth and co-workers[19−21] reported several experimental results on the comparison of ABA and BAB types of poly(oxyalkylene) triblock copolymers with nearly the same overall compositions and chain lengths in aqueous solutions. They found that the ABA triblock copolymer more easily forms the micelles at lower concentration compared to BAB triblock copolymer of the same composition in an aqueous solution selective for block A. Quintana et al.[22,23] investigated the association behavior of a triblock copolymer polystyrene-*b*-poly(ethylene/butylene)-*b*-polystyrene (SEBS) dissolved in a mixed selective solvent, where one solvent is selective for the outer blocks (i.e., polystyrene) and the other selective for the middle block (i.e., poly(ethylene/butylene)). They showed that SEBS triblock copolymer exhibits very different association behavior in the solvent mixture, depending on the composition of solvent mixture. On the other hand, Linse[15] has used the lattice self-consistent-field theory to theoretically calculate the effects of block architecture on the association behavior of ethylene oxide/propylene oxide block copolymer system. Very recently, Monzen et al.[24] also investigated the structures and the phase behavior of micelles prepared from symmetric and asymmetric triblock copolymers with different architecture, using the self-consistent-field theory. Their results showed that asymmetry between the two end blocks as well as block architecture strongly affects the micellization behavior in triblock copolymer solutions.

In this work, we directly compared the micelle formation and micellar parameters of ABA and BAB types of triblock copolymers to investigate the effects of block architecture in more detail by means of the computer simulation. As the computer simulation is based on the well-defined model, it can preclude the problems arising from the heterogeneities in chain composition and chain length that are unavoidable in experiments. Moreover, it proceeds straightforwardly without preassumptions

* To whom correspondence should be addressed. Tel +82-2-880-7192; Fax +81-2-885-1748; e-mail whjpoly@plaza.snu.ac.kr.

10.1021/ma0105136 CCC: $20.00
Published on Web 08/23/2001

of micelle geometry and chain conformation that are very often needed in the theoretical treatment. These advantages of simulation over the experiment and theory can make it possible to obtain direct and detailed knowledge on the similarities and differences of association behavior between the two different triblock copolymers. Several simulation studies on the micellization of block copolymers including diblock have been reported.[16,17,25−27] The detailed reviews on the simulation works can be found in refs 28 and 29. Unlike earlier simulation works, we use here the grand-canonical Monte Carlo (GCMC) simulation method to investigate the micellization of triblock copolymers. This GCMC technique has several advantages in studying the micellization behavior of amphiphilic molecules over the simulations based on the canonical ensemble, such as the use of smaller simulation box, faster equilibration of micellar size distribution, and so on.[29−31] In addition, with the knowledge of the chemical potential μ, the fundamental properties of the system such as the relative free energy or the entropy can be estimated. These properties are combined with the histogram reweighting method of Ferrenberg and Swendsen[32,33] to give us very useful information on the basic micellar parameters. Taking full advantage of GCMC method, we will obtain the micellar parameters such as the critical micelle concentration (cmc), the micellar association number, its association number distribution, and the standard thermodynamics of micellization. On the basis of these results, the similarity and difference in the micellization behavior between two different triblock copolymer and their mechanism of micellization will thoroughly be analyzed in terms of micellar parameters, which is very difficult to obtain from experiments and conventional canonical simulations.

2. Model and Simulation Method

All the simulations are performed on a cubic lattice using a Metropolis algorithm within the grand canonical ensemble (constant μVT ensemble). The linear dimension L of a simulation box is $L = 40$, and periodic boundary conditions are applied in three principal directions. The simulation model is designed to represent a solution of a solvent (selective for block A) and a triblock copolymer (ABA or BAB), where each segment of triblock copolymer occupies only single lattice site and all unoccupied sites are considered as solvents. Connected sites along copolymer backbone are determined by a vector of the basic set {(1,0,0), (1,1,0), (1,1,1)}, resulting in a coordination number of 26. All pairwise interactions ϵ are applied along the vector derived from the same basic set as above. The interaction ϵ_{BB} between B−B segments is chosen to be negative, and all the other interactions are set to be zero, i.e., $\epsilon_{AA} = \epsilon_{AB} = \epsilon_{AS} = \epsilon_{BS} = \epsilon_{SS} = 0$, where subscripts A, B, and S denote block A, block B, and solvent segments, respectively. This set of interactions induces the solvent to be selective for block A and therefore makes the block B form the core of micelles. In this work, ϵ_{BB} is set to be -1. The total chain length s of triblock copolymer is kept constant as $s = 30$ for both ABA and BAB. The lengths of each block are set to be $s_A = 10$ and $s_B = 10$ for ABA and $s_A = 20$ and $s_B = 5$ for BAB. We consider only symmetric triblock copolymers, and thus both types of triblock copolymer have the same composition (i.e., A/B = 2/1). A copolymer chain is designated as the chain belonging to a micelle if any segment of block B is in contact with any segment of block B of another chain.

The GCMC simulations are carried out in the conventional manner,[30,31] where the chemical potential, volume, and temperature of the system are kept constant while the density of the system is allowed to fluctuate throughout the simulation. In our simulation, the chain configurations are sampled by means of mixed moves of 50% chain displacement steps via reptation moves and 50% chain insertion/deletion steps within the grand canonical ensemble. It is very important that the acceptance probability of trial moves by which the chains are added or removed must be reasonable in order to become an efficient GCMC simulation. However, the GCMC simulation for chain molecules are extremely difficult, since the probability of inserting a polymer chain into a many-chain system without overlapping with existing chains is vanishingly small. The configurational bias Monte Carlo (CBMC) method is employed to facilitate the chain insertions and deletions in the grand canonical simulation. The essential idea behind the CBMC method is to improve the low acceptance rate associated with random trial chain insertion, by "growing" chains of favorable energy into the system.[31,34,35] A bookkeeping scheme maintains a record of the statistical bias associated with choosing favorable chain conformations, and this bias is subsequently removed when the acceptance probability is calculated. A more detailed description is given in refs 31 and 34.

In present work, the system temperature is systematically changed to investigate its effects on the micellization behavior in both types of triblock copolymer systems. At a given temperature, the chemical potential is scanned to check whether the system forms micelles at that temperature. For comparison, both ABA and BAB triblock copolymers are simulated at the same temperature, although they will have quite different critical micelle temperature (cmt) with each other.

3. Results and Discussion

As mentioned above, the chemical potential and the temperature of triblock copolymer systems are given as input parameters on the grand canonical ensemble, and correspondingly the average volume fraction of triblock copolymers in the system will be obtained through the simulation. In the following, we present our simulation results on the association behavior of both classes of triblock copolymers in a selective solvent as a function of their average volume fraction and temperature without specifying the chemical potential of the system.

Basic Micellar Parameters. Typical data for the distribution of association number for both types of ABA and BAB copolymers at different average volume fractions are shown in Figure 1, where the solvent is selective for block A and the temperature is $T = 4.5$. Here, the association number directly corresponds to the micellar size. Both triblock copolymers clearly exhibit a bimodal distribution of the association number at volume fractions above some critical one, which is a good evidence for the formation of thermodynamically stable micelle. Comparison of Figure 1a,b shows that there is a large difference in the critical concentration where the system shows the bimodal distribution between the two block copolymers, although they have the same chain length and composition. Judging from the size distribution curve, the cmc of ABA copolymer lies in the concentration range 0.0097−0.0198, while that of BAB copolymer lies in the range 0.0551−0.0790. This result is qualitatively consistent with the experimental ones

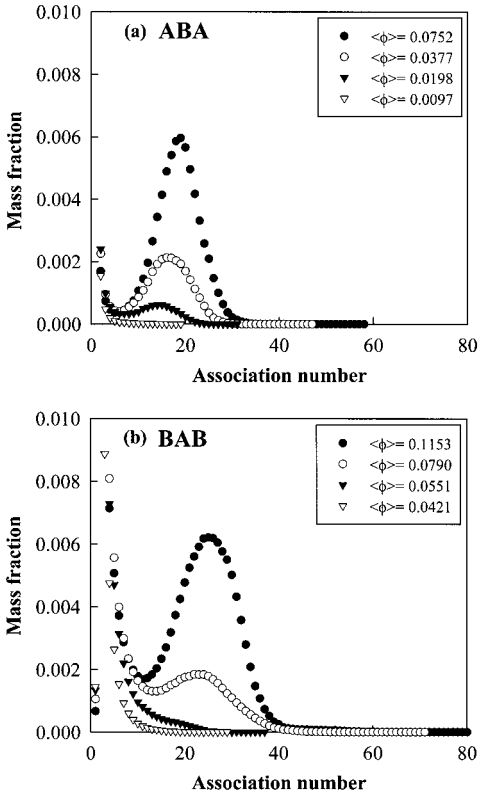

Figure 1. Mass fraction of micelles as a function of the association number when ABA (a) and BAB (b) block copolymers are micellized at various average volume fraction of copolymers at $T = 4.5$.

for triblock copolymers in organic or aqueous solutions,[18−21] implying that the ability to self-associate into micelles is considerably reduced for BAB copolymers as compared to ABA. This behavior can be ascribed to the additional entropy loss of BAB copolymer chains due to the looping geometry of the middle block because both end blocks should stay in the same micellar core to form micelles. A closer examination shows that the micelles of BAB copolymer formed at relatively high concentration are much larger in size and much broader in its distribution than ABA. We could even observe the micelles with the size of more than 80 (not shown here). The association behavior shown in Figure 1 is clearly different from the phase separation into the solvent- and copolymer-rich phases, because the micellar size distributions form a peak at high association number and are invariant throughout the simulation.

The effects of temperature on the association number distribution can be observed in Figure 2, where Figure 2a,b corresponds to $T = 4.4$ and $T = 4.7$ for ABA and Figure 2c,d to $T = 4.4$ and $T = 4.7$ for BAB, respectively. As expected, as the temperature decreases, the bimodal distribution of the micellar size starts to appear at lower concentration. This behavior implies that the micellization process is enthalpy driven. The micelles with low association number (which is here defined as small aggregate) become less significant with decreasing the temperature. This means that the free energy of triblock copolymer in a micelle becomes much lower than in free solution at lower temperature. As in the case in Figure 1, the micellar size of BAB is larger, and its distribution becomes much broader than ABA. This behavior may be related to unusual micellization behavior of BAB triblock copolymers due to their architecture, which will be discussed later.

For direct comparison of the micellar size and its distribution of ABA and BAB systems, the mean micellar sizes and their polydispersity are calculated and presented in Figures 3 and 4, respectively. The mean micellar sizes are defined as the weight-average association number N_w obtained from the association number distribution. Figure 3 clearly shows that BAB copolymer forms the micelles of much larger size than ABA. It can also be seen that the mean micellar size depends on the temperature, especially for ABA copolymers. The polydispersity of size is often expressed as the ratio of the weight-average association number N_w to the number-average association number N_n. It is clear that the polydispersity for BAB is larger than that for ABA at high concentration above the cmc, as shown in Figure 4. It is also observed that its dependence on the copolymer concentration behaves differently. With increasing the concentration, the polydispersity of ABA initially increases, shows a maximum, and then begins to decrease at some concentration above the cmc, as shown in Figure 4a. This behavior is explained as follows: at low concentration below the cmc, small aggregates with small association number predominantly forms, leading to narrow polydispersity. When the concentration reaches just above the cmc, the small aggregates coexist with the micelles that begin to form with relatively large association number, which results in broad polydispersity. As the copolymer concentration further increases, the fraction of micelles increases and their contribution becomes dominant. Consequently, the polydispersity becomes narrow again. Unlike ABA, the polydispersity of BAB is narrow below the cmc, and it continues to increase above the cmc and finally levels off. In the case of BAB, a considerable amount of small aggregates are present even after micelle formation due to the less capability to self-associate into micelle. Besides, various conformations of BAB copolymer chain in the micelle can lead to the formation of the micelles with sizes much higher than the mean micellar size. This behavior implies that the micellization process of BAB copolymer is closer to open association in nature.

To visualize the structure of micelles, snapshot pictures of the ABA and BAB micellar solutions are shown in Figure 5. ABA copolymers with the middle block B forming the core form the micelles with typical core−shell structure, as shown in Figure 5a where $T = 4.4$ and $\langle\phi\rangle = 0.0408$. Such micellization is known to obey the closed association model, yielding relatively narrow distribution of the micellar size, as observed in Figure 4a. Closer examination of single micelle formed from ABA reveals that the micelle formed is nearly spherical. In Figure 5b where $T = 4.3$ and $\langle\phi\rangle = 0.0455$, it can be seen that BAB copolymers with two end B blocks forming the micellar core yield micelles with broad size distribution, which may be characteristic of the open association. Most copolymer chains in the micelle takes a loop conformation, and part of the micelles exists as the so-called dangling chain which has one end in the core and the other in the solution. As the copolymer concentration increases, these free end blocks can participate in the core of another micelle or self-associate into new micelles, resulting in the branched or gel-like structure with bridge chains. Indeed, a number of bridge chains are observed at high concentration. These features of the micellization of BAB copolymers lead to loose or open structure with relatively broad distribution and large micellar size. Nev-

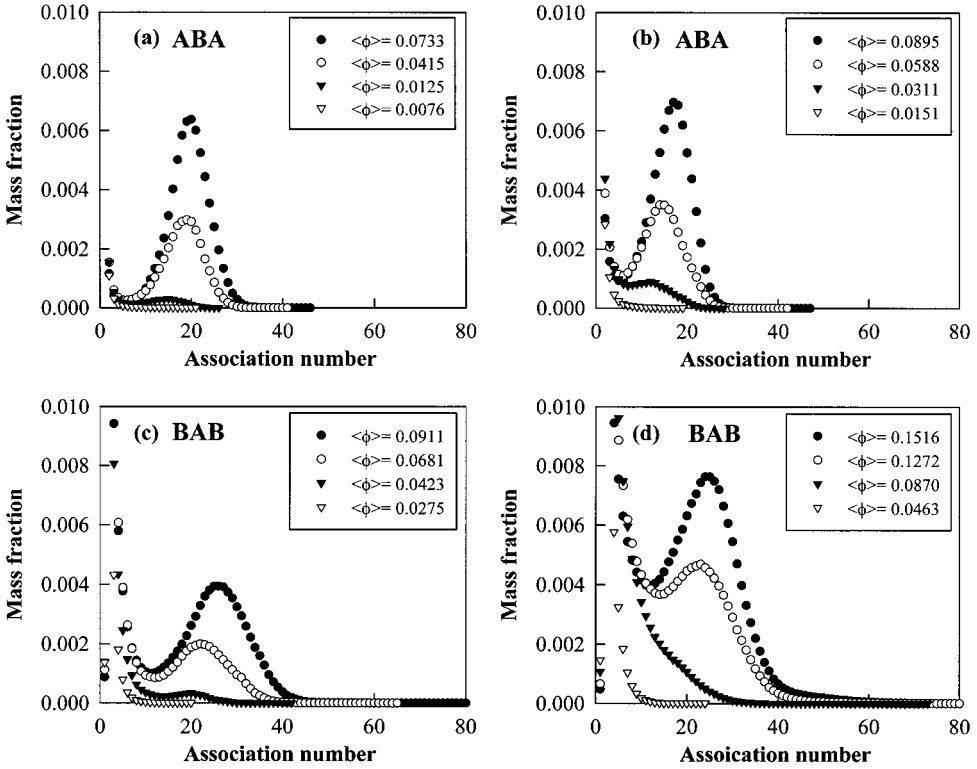

Figure 2. Effects of temperature on the micellization of ABA and BAB systems: (a) $T = 4.4$ for ABA; (b) $T = 4.7$ for ABA; (c) $T = 4.4$ for BAB; (d) $T = 4.7$ for BAB.

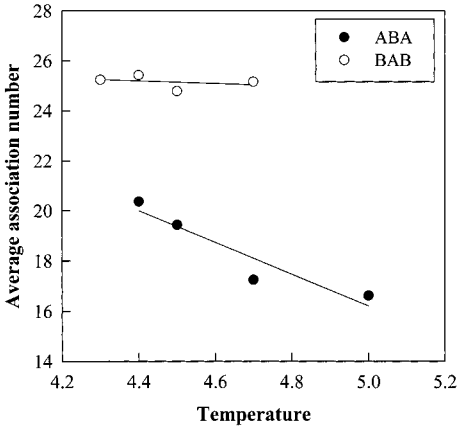

Figure 3. Change of the mean micellar size with temperature for ABA and BAB systems.

ertheless, the micelles formed from BAB copolymers are also found to be relatively spherical.

It is informative to analyze the status of copolymer chains such as free, dangling, loop, bridge chains as a function of concentration. For ABA, the copolymer exists either in a micelle or in a solution. As shown in Figure 6a, the fraction of free chains decreases with increasing the copolymer concentration. For BAB, the copolymer chain exists as one of four states, namely, free, dangling, loop, and bridge chain (see Figure 5b). As shown in Figure 6b, the fraction of free chain rapidly decreases with the concentration, as in the case of ABA. At low concentration, the fraction of dangling chain is larger than those of the loop and bridge chains. This is because the copolymer chains are not able to form a thermodynamically stable micelle but form small aggregates below the cmc. As the concentration increases, the fraction of dangling chains shows a maximum around the cmc and then decreases, implying the formation of

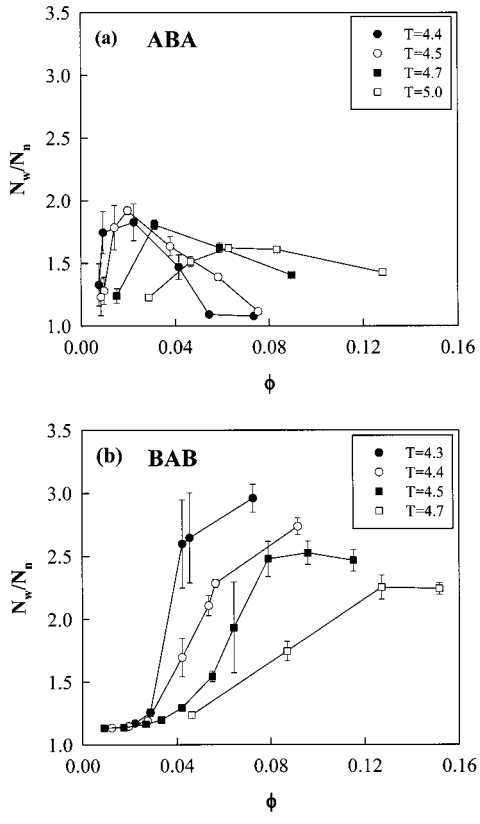

Figure 4. Dependence of polydispersity of the micellar size on the average volume fraction at various temperatures for (a) ABA and (b) BAB triblock copolymers.

the typical micelles. The fractions of loop and bridge chains steadily increase as the concentration increases, since they contribute significantly to the formation of the micelles. These relative fractions of chains strongly depend on the temperature at the concentration above

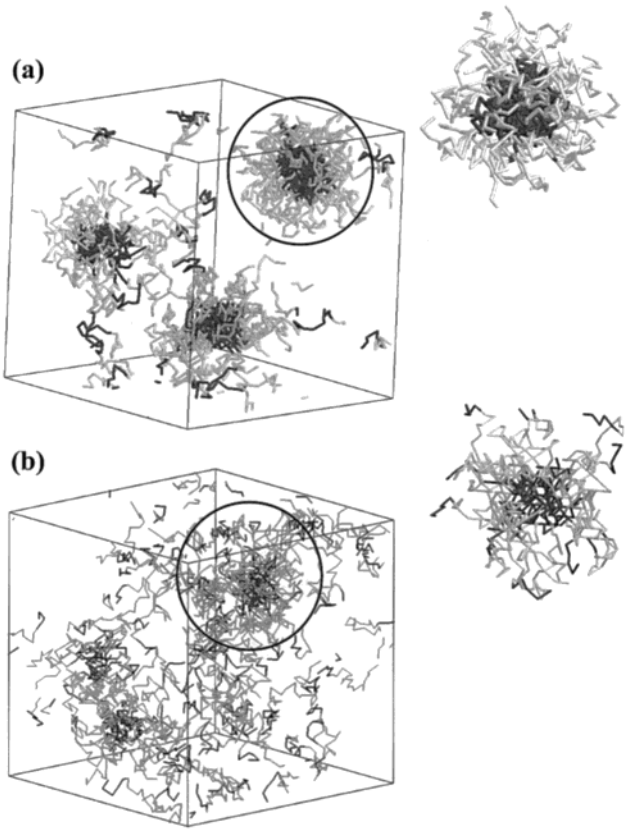

Figure 5. Snapshot pictures of the micellar system for (a) ABA at $T = 4.4$ and (b) BAB at $T = 4.3$. Each enlarged micelle corresponds to a circle in the respective picture.

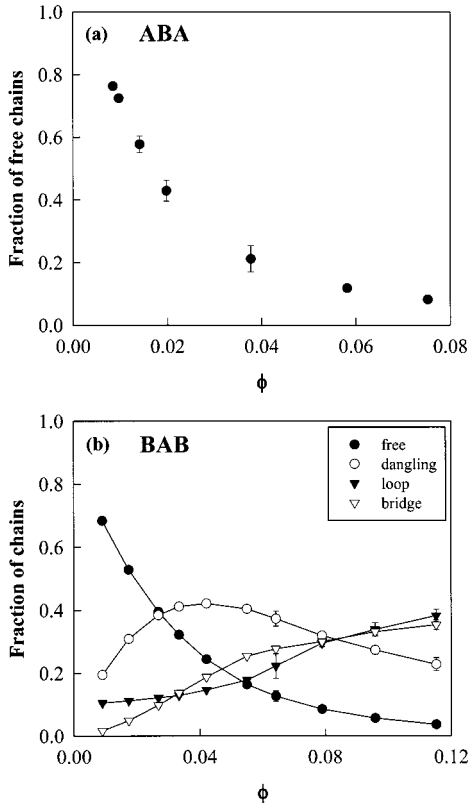

Figure 6. Change of the fraction of each conformation with the average volume fraction for (a) ABA and (b) BAB copolymers at $T = 4.5$.

the cmc (not shown here). As the temperature increases, the enthalpic interaction becomes less important, and as a result the fraction of dangling chains increases since unfavorable interaction of free ends in dangling chains becomes less significant. This increase in the fraction of dangling leads to the increase in the bridge fraction, since the bridge chain can be generated from the dangling chains. Accordingly, the population of loop chains with high entropic penalty decreases with increasing the temperature.

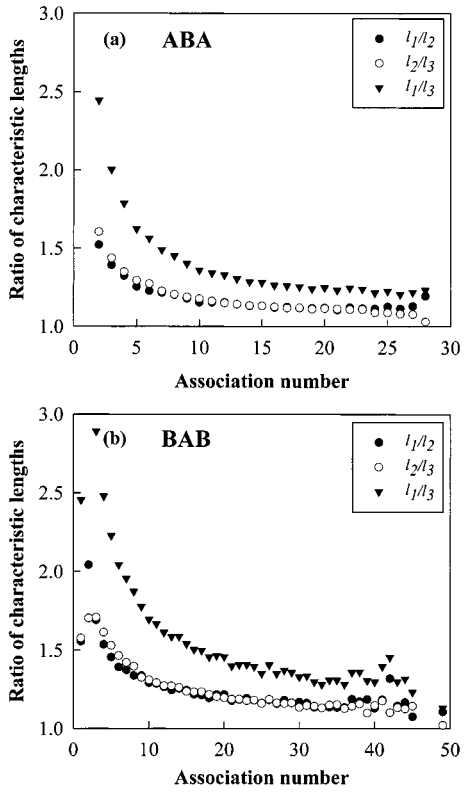

Figure 7. Ratio of characteristic lengths as a function of the association number for (a) ABA and (b) BAB copolymers at $T = 4.5$.

The shape of micelle can be quantitatively characterized by analyzing the principal moments of inertia of micelle. From the snapshot picture in Figure 5, it was realized that the shape of micelles is roughly spherical for both ABA and BAB. The set of eigenvalues (λ_1, λ_2, and λ_3; $\lambda_1 > \lambda_2 > \lambda_3$) of the moment of inertia matrix is evaluated, and a characteristic length is determined to be $l_i = \lambda_i^{1/2}$ for $i = 1, 2, 3$. A measure of the micellar asphericity, which is dependent on the micellar size, can be obtained by measuring l_1/l_2, l_2/l_3, and l_1/l_3. For a spherical micelle, $l_1/l_2 = l_2/l_3 = l_1/l_3 = 1$, and for a cylindrical one, $l_1/l_3 \gg 1$, $l_2/l_3 = 1$. When the ratios of characteristic lengths are plotted against the association number, it is observed that the characteristic length ratios are less than 2 for most of micelles except the small aggregates and becomes constant at large association number, indicating that the micelles formed by both types of triblock copolymers are nearly spherical.

Figure 8 shows the spherically averaged radial volume fraction profiles. For both cases, the micelle exhibits a typical radial distribution of spherical micelle, in which a dense core exclusively containing the segments B is surrounded by a less well-defined corona containing the segments A. Both triblock copolymers seem to have almost the same core radius of about 4.2 in our unit. However, a closer examination of Figure 8b shows that the BAB copolymer yields a long tail in the distribution of segment B extending into much outer region of the

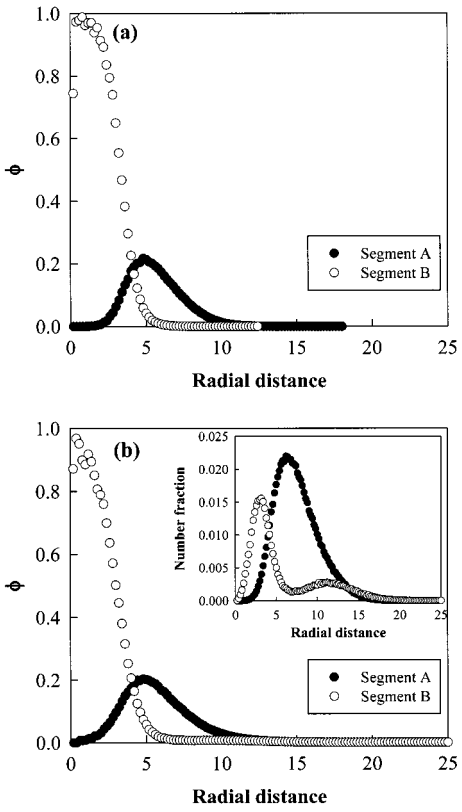

Figure 8. Spherically averaged radial density distribution function of micelles of (a) ABA with the association number $N = 18$ and (b) BAB with the association number $N = 23$ at $T = 4.5$.

micelle. This may be attributed to the peculiar topologies of BAB copolymers in the micelle such as the dangling and bridge, as shown in Figure 6. When the number fraction is used instead of volume fraction, it is clearer that the distribution of segment B shows the second peak in the outer region of micelle, in addition to the primary peak in the core region. It is believed that the B segments in the dangling and bridge chains contribute to this second peak in the radial distribution.

Critical Micelle Concentration (cmc). The critical micelle concentration (cmc) is generally defined as the concentration at which micelles first appear in solution at a given temperature. Here the exact values of the cmc for both systems are determined by calculating the osmotic pressure from the GCMC simulation combined with the multiple histogram method. The key idea of the histogram method, which was proposed by Ferrenberg and Swendsen,[32,33] is to increase the amount of information to improve the simulation efficiency. In the case of the single histogram method, the data from a single simulation at a given parameter set are extrapolated to give predictions of observable quantities at other parameter sets. The multiple histogram method allows us to interpolate/extrapolate the data from different simulations performed at different parameter sets to predict quantities over a wide range of parameter values.[36] For this purpose, in GCMC simulation at a fixed chemical potential μ and temperature T, the number of chains n and energy E are collected in the form of histogram. In this case, the grand canonical partition function Z is given as

$$Z(\mu,V,\beta) = \sum_n \sum_E W(n,V,E) \exp(\beta\mu n - \beta E) \quad (1)$$

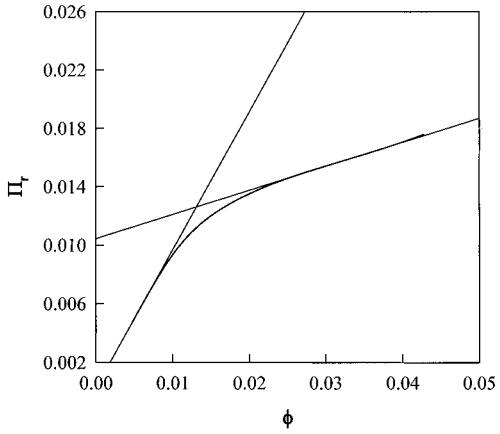

Figure 9. Reduced osmotic pressure as a function of the volume fraction of ABA triblock copolymer at $T = 4.5$. The cmc is determined as the concentration at which two straight lines intersect.

where $W(n,V,E)$ is the microcanonical partition function which is related to the entropy, and $\beta = 1/kT$. Then the probability $p(n,E)$ to observe a given number of chains n and energy E is as follows:

$$p(n,E) = W(n,V,E) \exp(\beta\mu n - \beta E)/Z(\mu,V,E) \quad (2)$$

The entropy, $S(n,V,E)$, can be estimated by a simple transformation of eq 2:

$$S(n,V,E)/k_B = \ln W(n,V,E) = \ln[p(n,E)] - \beta\mu n + \beta E + C \quad (3)$$

where C is an additive constant for the range of densities and energies covered in simulation. The multiple histogram method can be used to combine several simulation runs at different chemical potentials and temperatures to yield an overall estimate for entropy function. Using this entropy function, thermodynamic properties can be calculated at any other chemical potential and temperature, and the grand canonical partition function is obtained as follows:

$$Z(\mu,V,\beta) = C' \sum_n \sum_E \exp[S(n,V,E) + \beta\mu n - \beta E] \quad (4)$$

where C' is an unknown constant. The logarithm of the grand canonical partition function corresponds to the product of pressure and volume for a system, from which the osmotic pressure Π is calculated.[37] The constant C' can be obtained by comparing low-density results to the equation of state for the ideal gas. The osmotic pressure calculated for the ABA system is plotted against the volume fraction of copolymers in Figure 9, where the osmotic pressure is expressed in a reduced form as $\Pi_r = s\Pi/T$ with $T = 4.5$. At low concentration, the osmotic pressure increases linearly with a slope of nearly unity as the volume fraction increases. The other straight line can be drawn at higher volume fraction, as shown in Figure 9. Since the cmc is not a thermodynamic phase transition, it is defined phenomenologically as the concentration at which the observed property shows a discontinuity. Therefore, the cmc value can be estimated from the intersection of two straight lines, as shown in Figure 9. This method is generally applied to determine the cmc in experiments, using various physical properties.[38] The cmc value of ABA estimated at $T = 4.5$ is 0.0125, which lies within the range predicted from the

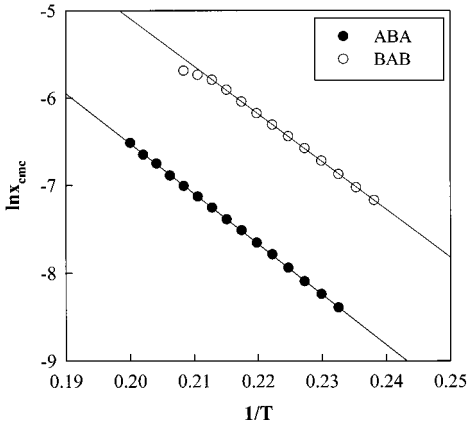

Figure 10. Logarithm of the critical micelle concentration as a function of the reciprocal temperature for ABA and BAB copolymer systems.

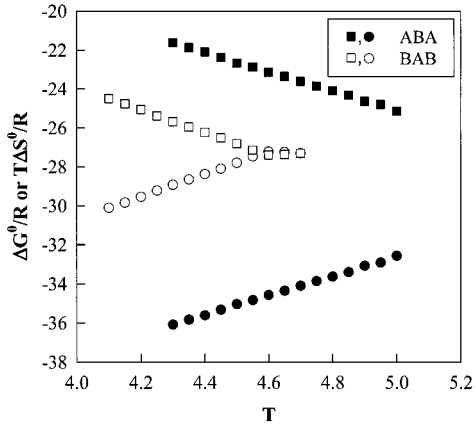

Figure 11. Standard free energy, $\Delta G°$ (●, ○), and standard entropy, $\Delta S°$ (■, □), as a function of temperature for ABA and BAB systems. The filled and open symbols correspond to ABA and BAB copolymer, respectively.

distribution curves of micellar size. The cmc values at other temperatures can be estimated with the same procedure. Furthermore, owing to the prediction by the multiple histogram method, the cmc values at other temperatures where the simulations have not been performed could also be estimated. As would be expected for a system with an enthalpic driving force for micellization, the cmc obtained increases with increasing the temperature. It is also confirmed that the cmc of BAB copolymer is much higher than that of ABA at a given temperature, as shown in Figure 10.

Thermodynamics of Micellization. In the previous section, we could obtain a well-defined cmc value for each system. Assuming that the association number is relatively large and has a narrow distribution, the closed association mechanism, where the micellization is characterized by a dynamic equilibrium between single copolymer chain and polymolecular micelle, predicts that the standard free energy and the standard enthalpy of micelle formation are related to the cmc, x_{cmc}, as follows:[3,38]

$$\Delta G° \approx -RT \ln K_c = RT \ln x_{cmc} \quad (5)$$

$$\Delta H° \approx -R[\mathrm{d} \ln K_c/\mathrm{d}(1/T)] = R[\mathrm{d} \ln x_{cmc}/\mathrm{d}(1/T)] \quad (6)$$

where x_{cmc} is expressed in mole fraction unit. The standard entropy of micelle formation is obtained by the relationship

$$\Delta S° = (\Delta H° - \Delta G°)/T \quad (7)$$

In principle, the standard state is copolymer molecules and micelles in an ideally dilute solution, and the values obtained are per mole of copolymer molecules. Under assumptions that the association number and $\Delta H°$ are independent of temperature, the integration of eq 6 gives

$$\ln x_{cmc} = \Delta H°/RT + \text{const} \quad (8)$$

When the logarithm of the cmc values for both systems are plotted against the inverse temperature, as shown in Figure 10, a straight line is obtained for both types of triblock copolymers, except for the cmc data of BAB at high temperatures. These results suggest that the micellization of the two triblock copolymers obeys the closed association model, although BAB copolymers exhibit some characteristics of open association due to the presence of dangling and bridge chains. The standard enthalpies of micellization, $\Delta H°$, estimated from the slope of Figure 10, are −57.7 and −54.6 kJ/mol for ABA and BAB, respectively. One of the assumptions in deriving above equations is that the micelle association number is large (generally $N > 50$) and independent of temperature. In all cases, our simulation results do not meet this assumption (see Figure 3). The correction for this disagreement can be performed in a standard manner.[3,14,21,39,40] The logarithmic values of $\Delta H°$ corrected were again fitted nicely by a straight line, yielding $\Delta H° = -60.3$ kJ/mol for ABA and $\Delta H° = -54.4$ kJ/mol for BAB. Nguyen-Misra and Mattice[16] have conducted canonical Monte Carlo simulations on the formation of micelle and gel of BAB triblock copolymers, which corresponds to a part of our model system. They calculated the relevant micellar and/or network parameters and investigated the effects of the degree of incompatibility between B segment and either A segment or solvent on the cmc and critical gel concentration. Their results for BAB triblock qualitatively showed very similar results on the basic micellization behavior to our case. However, according to their simulation results, the cmc of BAB copolymers was found to exhibit a weaker dependence on the incompatibility as compared with the exponential dependence in our case, i.e., $x_{cmc} \sim (2s_B\epsilon/kT)^{-0.4}$, due to the larger entropic penalty associated with triblock copolymers. It may be thought that this apparent discrepancy is attributed to the large difference in the block composition. Their BAB chains have longer total length of insoluble block B than that of block A whereas $2s_B < s_A$ in our case. Therefore, their BAB copolymer may experience much stronger entropic effects upon micellization. In fact, most experimental results for BAB triblocks with longer soluble block showed the same dependence as our case.[8,10,20−23] Figure 11 shows the calculation results for $\Delta G°$ and $\Delta S°$ for both systems. $\Delta G°$ is negative for both systems and becomes more negative as the temperature decreases. It is also observed that the ABA copolymer has more negative values than BAB over all temperatures simulated, indicating that the micellar solution of ABA copolymer is more stable and therefore has a lower cmc value. $\Delta H°$ and $\Delta S°$ also show the negative values for both copolymer systems, implying that the micellization is an enthalpy-driven process. When the entropy of micellization of BAB is compared with that of ABA, it is revealed that the entropy loss of BAB is larger than

that of ABA. This indicates that BAB copolymers require the looping geometry with high entropy penalty for micelle formation, and thereby some of them should be in the form of dangling chains in micelles, leading to unfavorable contacts between segment B and solvent. This unfavorable contact leads to less negative value of $\Delta H°$ for BAB than ABA.

Thermodynamic analysis for the micellization of two copolymers shows that BAB copolymers have higher cmc values than ABA. However, as shown in Figure 3, the mean association number of BAB, despite its higher cmc, is larger than that of ABA. In this section, we attempt to explain this behavior through a more rigorous approach. Indeed, the model derived above suffers a serious limitation in that it considers only one species of micelles; i.e., it assumes monodispersity of the micellar size. The obvious extension of such a model is to introduce micelles of different sizes which are in equilibrium with each other. This multiple equilibrium model can not only predict the size distribution in the micellar solution but also extract the entropy associated with packing the chains into a micelle, which controls the micellar size, as presented in very recent work of Care and Dalby.[41] According to the multiple equilibrium model, the micellar size distribution can be obtained as below:[38,41]

$$x_N = N \frac{(a_1 x_1)^N}{a_N} \exp\left[-N \frac{\mu_N^0 - \mu_1^0}{kT}\right] \qquad (9)$$

where x_N is the mole fraction of chains present in micelles with association number N, μ_i^0 the chemical potential per molecule in a micelle of size i in a dilute reference state, and a_i an activity coefficient. The activity coefficient can be estimated from the second virial coefficient between two micelles following the approach proposed by von Gottberg et al.[42] At low concentrations, the micelle−micelle interaction may be ignored and thus the excess chemical potential per molecule can be given as[41]

$$\frac{\mu_N^0 - \mu_1^0}{kT} = \frac{1}{kT}\left(\frac{\bar{U}^N}{N} - \bar{U}^1\right) - \frac{1}{k}\left(\frac{S^N}{N} - S^1\right) \qquad (10)$$

The excess chemical potential per molecule ($\mu_N^0 - \mu_1^0$) can be calculated from the micellar size distribution using eq 9. The potential energy $\bar{U}^N$ for a micelle of size N is also calculated during the simulation, and therefore the excess enthalpy per molecule, $[(\bar{U}^N/N) - \bar{U}^1]/kT$, can be estimated directly from the simulation. The last term $[(S^N/N) - S^1]/k$ is the excess entropy per molecule, and the entropic terms related to the translation of the micelles cancel out in eq 10. Therefore, S^N is regarded as the entropy associated with packing the chains into the micelle.[41] Figure 12 compares the excess thermodynamic properties of ABA with those of BAB under the same condition of micellization. The excess chemical potential of ABA is slightly lower than BAB, indicating that the micellization of ABA triblock copolymers is more favorable. This arises mainly from a large difference in the excess enthalpy per molecule. The reason that BAB copolymer shows much less negative excess enthalpy per molecule is that the micelles of BAB copolymer yield loose or open structure through dangling and bridge chains. This has already been identified in the case of $\Delta H°$. Such imperfect structure of micelles of BAB copolymers, however, gives much lower packing entropy of their micelles than those of ABA, as shown in Figure 12. As the micellar size increases, this packing entropy of chains in micelles decreases and eventually limits further growth in the micelle size due to an increased self-crowding at the micellar surface. Therefore, BAB copolymers with smaller decrease in the excess entropy per molecule may form the micelles with larger size than ABA.

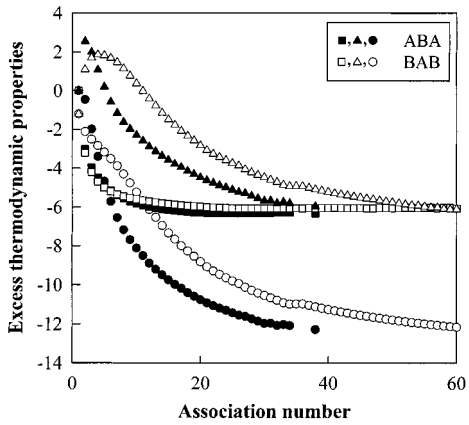

Figure 12. The excess enthalpy (●, ○), the excess chemical potential, (■, □), and the excess entropy (▲, △) per copolymer chain as a function of the micellar size. The filled and open symbols correspond to ABA and BAB system, respectively.

4. Conclusions

In this work, the micellization behavior of two ABA and BAB triblock copolymers in a selective solvent for block A has been compared through the grand canonical Monte Carlo simulation combined with the histogram method. Our simulation model successfully generated the spherical micelles for both types of triblock copolymers, and cmc values were also determined unambiguously. It was found that BAB triblock copolymers in a solvent selective for the middle block show much higher cmc values at the same temperature than ABA in a solvent selective for two end blocks, exhibiting a large reduction of the capability of BAB triblock copolymers to self-assemble. This difference in the micellization behavior arises from an additional entropy penalty associated with looping conformation of the middle block of BAB copolymers. This looping conformation is directly observed from snapshot picture and also supported by thermodynamic analysis of micelle formation. Moreover, the entropy penalty for BAB copolymers leads to the micellar structure with significant fraction of dangling and bridge chains. The presence of dangling chains is directly identified from the radial density distribution of chains in micelles and induces a decrease in the standard enthalpy of micellization as compared with the case of ABA copolymers. Nevertheless, the presence of well-defined cmc and the results of thermodynamic analysis indicate that both triblock copolymers follow the closed association mechanism, although BAB copolymer shows some characteristics of open association through the molecular and micellar linking by dangling and bridge chains. One of the differences between ABA and BAB copolymers is that BAB copolymers form the micelles with larger size and broader size distribution than ABA, despite their reduced ability to self-assemble into micelles. The multiple equilibrium model was used to extract the entropy associated with packing the chains into a micelle from our simulation results. BAB copolymers with larger micellar size and broader size

distribution are found to have much lower packing entropy than ABA copolymers. Considering that this packing entropy limits the growth of micellar size, it is easily understood that BAB copolymers form the micelles with larger size and broader size distribution than ABA.

In this paper, the micellization behavior for two classes of block copolymers with single composition has extensively been analyzed. However, since it is expected that the micellization strongly depend on the copolymer composition, the effects of the composition of both types of triblock copolymers on micellization will be reported in the next paper.

Acknowledgment. The authors thank the Korea Science and Engineering Foundation (KOSEF) for their financial support through Hyperstructured Organic Materials Research Center (HOMRC).

References and Notes

(1) Brown, R. A.; Masters, A. J.; Price, C.; Yuan, X. F. In *Comprehensive Polymer Science*; Booth, C., Price, C., Eds.; Pergamon: Oxford, 1989; Vol. 2, p 155.
(2) Chu, B.; Zhou, Z. In *Nonionic Surfactants, Polyoxyalkylene Block Copolymers*; Nace, V. N., Ed.; Marcel Dekker: New York, 1996; Vol. 60.
(3) Hamley, I. W. In *The Physics of Block Copolymers*; Oxford University: New York, 1998; p 131.
(4) Alexandridis, P.; Holzwarth, J. F.; Hatton, T. A. *Macromolecules* **1994**, *27*, 2414.
(5) Raspaud, E.; Lairez, D.; Adam, M.; Carton, J.-P. *Macromolecules* **1994**, *27*, 2956.
(6) Mortensen, K.; Brown, W.; Jorgensen, E. *Macromolecules* **1994**, *27*, 5654.
(7) Zhou, Z.; Chu, B.; Nace, V. M.; Yang, Y.-W.; Booth, C. *Macromolecules* **1996**, *29*, 3663.
(8) Quintana, J. R.; Janez, M. D.; Katime, I. *Langmuir* **1997**, *13*, 2640.
(9) Nolan, S. L.; Phillips, R. J.; Cotts, P. M.; Dungan, S. R. *J. Colloid Interface Sci.* **1997**, *191*, 291.
(10) Quintana, J. R.; Janez, M. D.; Katime, I. *Polymer* **1998**, *39*, 2111.
(11) Quintana, J. R.; Diaz, E.; Katime, I. *Langmuir* **1998**, *14*, 1586.
(12) Keki, S.; Deak, G.; Kuki, A.; Zsuga, M. *Polymer* **1998**, *29*, 6053.
(13) Liu, T.; Zhou, Z.; Wu, C.; Nace, V. M.; Chu, B. *J. Phys. Chem. B* **1998**, *102*, 2875.
(14) Booth, C.; Attwood, D. *Macromol. Rapid Commun.* **2000**, *21*, 501.
(15) Linse, P. *Macromolecules* **1993**, *26*, 4437.
(16) Nguyen-Misra, M.; Mattice, W. L. *Macromolecules* **1995**, *28*, 1444.
(17) Nguyen-Misra, M.; Mattice, W. L. *Macromolecules* **1995**, *28*, 6976.
(18) Zhou, Z.; Chu, B. *Macromolecules* **1994**, *27*, 2025.
(19) Yang, Z.; Pickard, S.; Deng, N.; Barlow, R. J.; Attwood, D.; Booth, C. *Macromolecules* **1994**, *27*, 2371.
(20) Yang, Y.-W.; Yang, Z.; Zhou, Z.-K.; Attwood, D.; Booth, C. *Macromolecules* **1996**, *29*, 670.
(21) Altinok, H.; Yu, G.-E.; Nixon, S. K.; Gorry, P. A.; Attwood, D.; Booth, C. *Langmuir* **1997**, *13*, 5837.
(22) Quintana, J. R.; Janez, M. D.; Katime, I. *Macromolecules* **1998**, *31*, 6865.
(23) Quintana, J. R.; Hernaez, E.; Inchausti, I.; Katime, I. *J. Phys. Chem. B* **2000**, *104*, 1439.
(24) Monzen, M.; Kawakatsu, T.; Doi, M.; Hasegawa, R. *Comput. Theor. Polym. Sci.* **2000**, *10*, 275.
(25) Nelson, P. H.; Rutledge, G. C.; Hatton, T. A. *J. Chem. Phys.* **1997**, *107*, 10777.
(26) Viduna, D.; Milchev, A.; Binder, K. *Macromol. Theory Simul.* **1998**, *7*, 649.
(27) Milchev, A.; Bhattacharya, A.; Binder, K. *Macromolecules* **2001**, *34*, 1881.
(28) Shelley, J. C.; Shelley, M. Y. *Curr. Opin. Colloid Interface Sci.* **2000**, *5*, 101.
(29) Binder, K.; Muller, M. *Curr. Opin. Colloid Interface Sci.* **2000**, *5*, 315.
(30) Allen, M. D.; Tildesley, D. J. In *Computer Simulation of Liquids*; Clarendon: Oxford, 1989.
(31) Frenkel, D.; Smit, B. In *Understanding Molecular Simulation*; Academic Press: New York, 1996.
(32) Ferrenberg, A. M.; Swendsen, R. H. *Phys. Rev. Lett.* **1988**, *61*, 2635.
(33) Ferrenberg, A. M.; Swendsen, R. H. *Phys. Rev. Lett.* **1989**, *63*, 1195.
(34) Smit, B. *Mol. Phys.* **1995**, *85*, 153.
(35) Wilding, N. B.; Muller, M.; Binder, K. *J. Chem. Phys.* **1996**, *105*, 802.
(36) Deutsch, H. P. *J. Stat. Phys.* **1992**, *64*, 1039.
(37) Floriano, M. A.; Caponetti, E.; Panagiotopoulos, A. Z. *Langmuir* **1999**, *15*, 3143.
(38) Attwood, D.; Florence, A. T. In *Surfactant Systems: Their Chemistry, Pharmacy and Biology*; Chapman and Hall: London, 1983.
(39) Yang, Y.-W.; Deng, N.-J.; Yu, G.-E.; Zhou, Z.-K.; Attwood, D.; Booth, C. *Langmuir*, **1995**, *11*, 4703.
(40) Kelarakis, A.; Havredaki, V.; Yu, G.-E.; Derici, L.; Booth, C. *Macromolecules* **1998**, *31*, 944.
(41) Care, C. M.; Dalby, T. *Europhys. Lett.* **1999**, *45*, 38.
(42) von Gottberg, F. K.; Smith, K. A.; Hatton, T. A. *J. Chem. Phys.* **1997**, *106*, 9850.

MA0105136